Journal of Hydroscience and Hydraulic Engineering
Vol. 28, No.2 November, 2010, 37-47

NUMERICAL PREDICTION METHOD FOR MULTIPHASE FIELDS TO PREDICT FLUID FORCES ACTING ON MULTIPLE RIGID CYLINDERS

By

Satoru Ushijima

ACCMS, Kyoto University, Kyoto-shi, 606-8501, Japan

Norimasa Yoshikawa

Aisin Seiki Co., Ltd., Asahi-machi 2-1, Kariya, Aichi, 448-8650, Japan

and

Genta Nakamura

CERE, Kyoto University, Kyoto-shi, 615-8540, Japan

SYNOPSIS

The applicability of a computational method was investigated to predict the fluid forces acting on multiple rigid cylinders in wave-induced flows. The free-surface flows including cylinders are treated as incompressible gas, liquid and solid fields in the computational method, MICS (Multiphase Incompressible flow solver with Collocated grid System), which is a solver for multiphase fields. The solid objects included in the flows are represented by tetrahedron elements. The areas occupied by the elements are modeled as the incompressible fluids which have the same densities as the solid objects. The basic equations for the modeled fluids are discretized with a finite volume method on a collocated grid system and they are solved with MAC procedures. The fluid forces against the objects are estimated with the volume integral of the momentum equations for the solid areas. The prediction method was applied to the experiments, in which a water tank equipped with multiple cylinders was accelerated in one direction and the fluid forces on the cylinders were measured by means of strain gages. As a result of the computations, it was confirmed that the predicted time-histories and peak values of the fluid forces are generally in good agreement with the experiments. By making comparisons with experimental results, the applicability of the computational method was discussed.

INTRODUCTION

Recently, it is one of the important hydraulics subjects to deal with the plants in a riparian zones, which is basically the interface between river bank and stream. The riparian vegetation along the river margins plays a significant role in ecology, environmental management as well as river hydraulics, since it has a close relation to aquatic ecosystems. In terms of the river engineering, the riparian vegetation sometimes causes flow resistance and resulting increase of water levels of flood flows. In addition, it is reported that the driftwood are occasionally trapped by the riparian plants and they cause large resistance against flood flows. The vegetation zone near

coastal regions, on the other hand, is utilized as the tidewater control forest to prevent wave-induced flows caused by storm surges and Tsunamis. In this case, the resistance force against flows is desired to be sufficiently large.

Considering the above situation, a computational method was investigated in the present study to establish an effective prediction method to estimate the fluid forces acting on multiple plants, which are simply represented by a group of rigid cylinders. Regarding the experimental studies for such problems, investigations have been carried out to understand the effects of plants on flow fields by measuring fluid forces affecting cylindrical models in open channel flows (1), measuring velocity profiles in arboreal vegetation models (2) and field observations for the velocity distributions in plants (3), (4) and (5).

In the present study, the applicability of a computational method, MICS (Multiphase Incompressible flow solver with Collocated grid System) (6), was investigated to estimate the fluid forces acting on multiple cylindrical objects in wave-induced flows. This method is based on a one-equation model for incompressible fluid-mixture and it enables us to deal with gas, liquid and solid phases by assuming that these phases are incompressible fluid-mixture. In order to confirm the applicability of this computational method, it was applied to hydraulic experiments, in which a water tank equipped with multiple rigid cylinders was accelerated and the fluid forces caused by the generated wave-induced flows were measured with strain gages. The validity of the computational method is examined by making comparisons between experiments and computations, regarding the time history of fluid forces and the relationship between the fluid forces and the number of cylinders.

NUMERICAL PROCEDURES

Governing equations for gas and liquid phases

The computational method for multiphase fields, MICS (6), is used to predict the fluid forces acting on the cylindrical objects in free-surface flows. In this method, the multiphase fields consisting of gas and liquid phases are firstly solved with the following equations:

$$\frac{\partial \rho_f}{\partial t} + \frac{\partial}{\partial x_j}(\rho_f u_j) = 0 \tag{1}$$

$$\frac{\partial u_j}{\partial x_j} = 0 \tag{2}$$

$$\frac{\partial u_i}{\partial t} + \frac{\partial}{\partial x_j}(u_i u_j) = f_i - \frac{1}{\rho_f}\frac{\partial p}{\partial x_i} + \frac{1}{\rho_f}\frac{\partial}{\partial x_j}\left[\frac{\partial}{\partial x_j}(\mu u_i) + \frac{\partial}{\partial x_i}(\mu u_j)\right] \tag{3}$$

where t is time, x_i orthogonal coordinates, f_i external acceleration component in the x_i direction and u_i mass-averaged velocity component of gas and liquid phases defined by

$$u_i = \frac{\sum_k \Omega_k \rho_k u_{k,i}}{\Omega \rho} \tag{4}$$

where subscript k stands for the specific phase$-k$ in the multiphase field. Ω is the considering volume of whole multiphase field and Ω_k is the volume of phase$-k$ included in Ω. The variables ρ_f, p and μ in Eqs. 1 and 3 represent the volume-averaged density in gas and liquid phases, pressure and viscous coefficient, respectively, which are defined as the follows:

$$\phi = \frac{\sum_k \Omega_k \phi_k}{\Omega \rho} \tag{5}$$

Here the variable ϕ denotes density, pressure or viscous coefficient in phase$-k$. The above governing equations are derived in the similar way to the one-fluid model used in multiphase flows (7).

The momentum equations given by Eq. 3 are discretized using a finite volume method in the collocated grid system which is fixed in the space. The SMAC algorithm (8) is used to solve the above governing equations for incompressible flows. In the prediction stage of the MAC procedures, an implicit method, C-ISMAC (9), is used to decrease computational time as well as to preserve computational accuracy, which is equivalent to fifth-order accuracy (10). In addition, in the pressure-computation stage, the C-HSMAC method (11) is employed to keep the error of fluid continuity sufficiently small in all fluid cells. It has been shown that the C-HSMAC method is much more efficient compared with the usual SOLA method (12).

Fluid forces acting on objects

In contrast to the usual computational methods in hydraulics that use empirical resistance and lift coefficients, the fluid forces acting on the objects are estimated in the present method more accurately through the pressure and viscous terms in momentum equations. Since the solid object is treated as an incompressible fluid, the momentum equation for the solid area can be written as

$$\frac{\partial u_i}{\partial t} + \frac{\partial}{\partial x_j}(u_i u_j) = -\frac{\rho_b - \rho_f}{\rho_b} g \delta_{3,i} - \frac{1}{\rho_b}\frac{\partial \phi^*}{\partial x_i} + \frac{1}{\rho_b}\frac{\partial}{\partial x_j}\left[\frac{\partial}{\partial x_j}(\mu u_i) + \frac{\partial}{\partial x_i}(\mu u_j)\right] \tag{6}$$

where g is gravity acceleration, x_3 vertical coordinate in upward direction and $\delta_{i,j}$ Kronecker's delta. The pressure deviation from the static pressure is denoted by ϕ^*. The variable ρ_b is the density evaluated with the mass of the solid object that occupies in a fluid cell and its value is determined by means of a tetrahedron sub-cell method (13). Thus, the solid object is represented with multiple tetrahedron elements and the volume fraction of each element included in an Eulerian fluid cell is approximated with the number of sub-cells that are created by subdividing it. The example of solid objects and their tetrahedron elements are shown in Fig. 1. The original shapes of the objects are generated with a commercial CAD software and then tetrahedron elements are set up with a mesh-generation software.

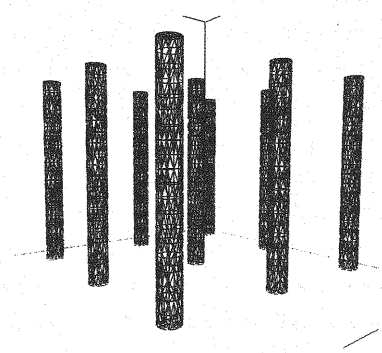

Fig. 1 Tetrahedron elements generated for cylinders

The fluid forces acting on the objects are determined from the right hand side of Eq. 6. As schematically shown in Fig. 2, the volume fraction of the element m of the object k that occupies in a fluid cell C is defined as α_{Ckm}, which is estimated with the sub-cell method. With the α_{Ckm}, the volume of C and ρ_b, the fluid force

component F^i_{Ckm} acting on the volume fraction is calculated from the following relationship:

$$F^i_{Ckm} = \alpha_{Ckm}\rho_b V_C \cdot RHS \tag{7}$$

where RHS stands for the right hand side of Eq. 6. By adopting the same procedures for all tetrahedron elements and fluid cells and taking the summation of them, fluid force F^i_k acting on object k is determined.

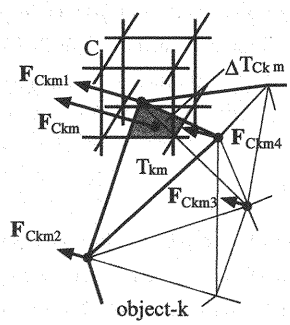

Fig. 2 Relationship between tetrahedron elements of object$-k$ and a fluid cell

APPLICABILITY OF COMPUTATIONAL METHOD

Experiments to measure fluid forces of wave-induced flows against cylinders

Hydraulic experiments were carried out to measure the fluid forces acting on multiple cylinders in wave-induced flows. Fig. 3 shows the schematic view of the experimental equipments. A water tank with the length $L = 300$ mm and width $B = 170$ mm is fixed on a moving plate connected with an electric slider whose acceleration can be controlled by a computer. In the tank, multiple cylinders are set up, whose top surfaces are fixed on a horizontal board as shown in Fig. 3 (b). The board is a square acrylic plate of each side length $b = 110$ mm and thickness 2 mm. In addition, this board is supported by a vertical steel plate, as shown in Fig. 4, on which four strain gages are attached to measure the fluid forces against the cylinders. The motions of the tank and the cylinders are mutually independent, since there is 2 mm clearance between the bottom ends of the cylinders and the bottom surface of the tank. The diameter of the cylinder D and its length l are 8 mm and 87 mm respectively. The distance d between the central axes of two adjacent cylinders is uniform in the x and y directions in all experiments. The numbers of cylinders in one direction, N_1, are 3, 4 and 5. The distance d is given by $100/(N_1 - 1)$ mm. Hereafter, the experimental condition is referred to case$-N_1 \times N_1$ when the number of cylinders is $N_1 \times N_1$. The total number of cylinders is denoted as N, which is equal to N_1^2.

In the experiments, the initial water depth h_0 in the tank was set at 50 mm and the initial distance L_0 in Fig. 3 (a) was 225 mm. After the acceleration of 1 m/s^2 was added to the tank during 0.224 sec. in the x direction, the negative acceleration -1 m/s^2 was then imposed on it during the same time period. Thus, the tank was stopped at 0.448 sec. after the start of the experiments. Large oscillations of water surface, or sloshing motions, and the resulting wave-induced flows arise in the tank during and after the acceleration. By adding this acceleration, the tank is actually moved about 50 mm in the x direction, which is denoted by x_0 in Fig. 3 (a), while the cylinders fixed on the external frames are still located in the initial position. This movement can be represented as the relative movements of the cylinders on the basis of the coordinates fixed on the tank.

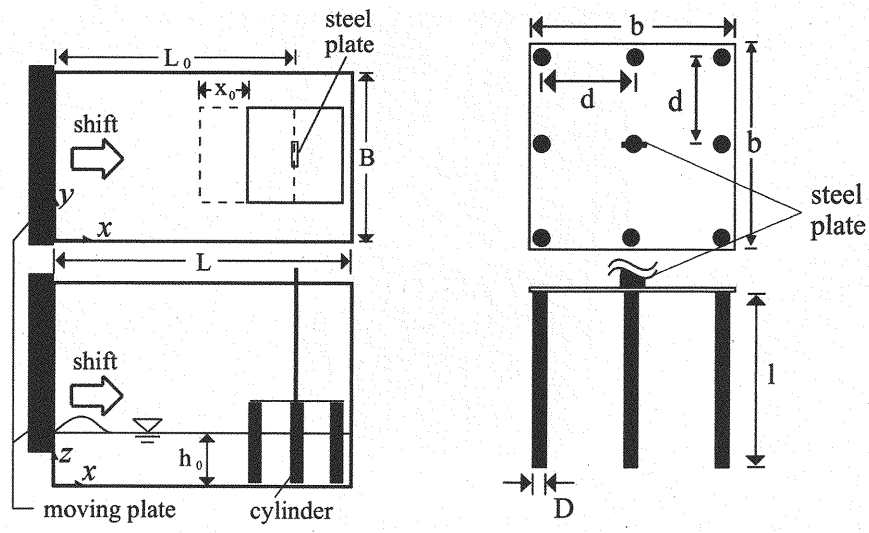

(a) Schematic view of experimental equipment (b) Arrangements of cylinders

Fig. 3 Experimental equipments

Conditions of computations

In the computations, $90 \times 60 \times 30$ computational cells are set up in the x, y and z directions respectively for the computational area of $300 \times 170 \times 150$ mm. This area includes water and air regions in the tank as well as the cylinders. In the calculations, each rigid cylinder was represented by 1,471 tetrahedron elements with 436 nodes as shown in Fig. 1. The conditions of the calculations were basically the same as those of the experiments. The kinematic viscosities of water and air were set at 1.0×10^{-6} and 1.0×10^{-5} m^2/s respectively. Their densities were 1.0×10^3 and 1.0 kg/m^3 similar to the experiments.

The motions of the tank are simulated by the relative movements of the cylinders and impositions of the corresponding horizontal acceleration. Thus, while the tank is stationary in the computations, the sloshing motions and wave-induced flows are exactly replicated by adding the same accelerations to the fluids in the tank and the same movements of the cylinders.

Computational results for rigid cylinders

Figs. 5 and 6 show the predicted free-surface profiles and velocity vectors on the horizontal section 5 mm above the bottom surface for the case−3×3 and case−5×5. These figures are snapshots at 0.7, 0.8, 0.9 and 1.0 sec., indicating the wave motions proceeding to left, or the $-x$ direction, which were reflected on the right wall. It can be seen that the existence of cylinders causes small disturbances on the water surface as well as the complicated flow patterns around cylinders. In the case−5×5, the proceedings of the wave motions are slightly slower than the case−3×3, due to the increase of the resistances of the cylinders.

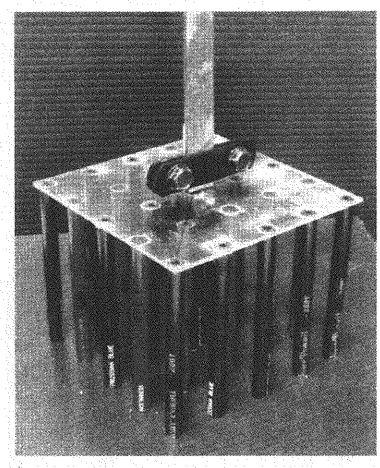

Fig. 4 Cylinders used in experiments (case−5×5)

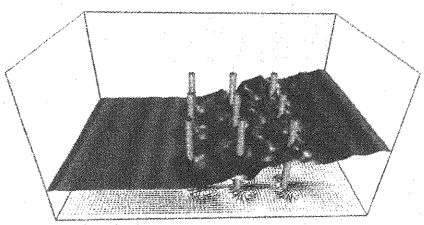

(a) $t = 0.7$ (s)

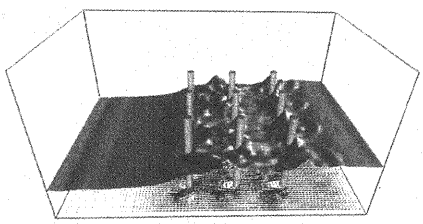

(b) $t = 0.8$ (s)

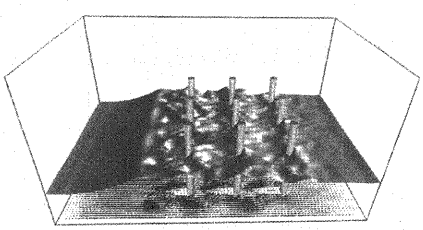

(c) $t = 0.9$ (s)

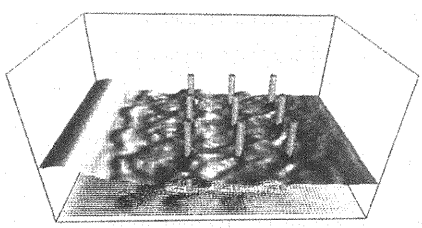

(d) $t = 1.0$ (s)

Fig. 5 Predicted results for case−3×3

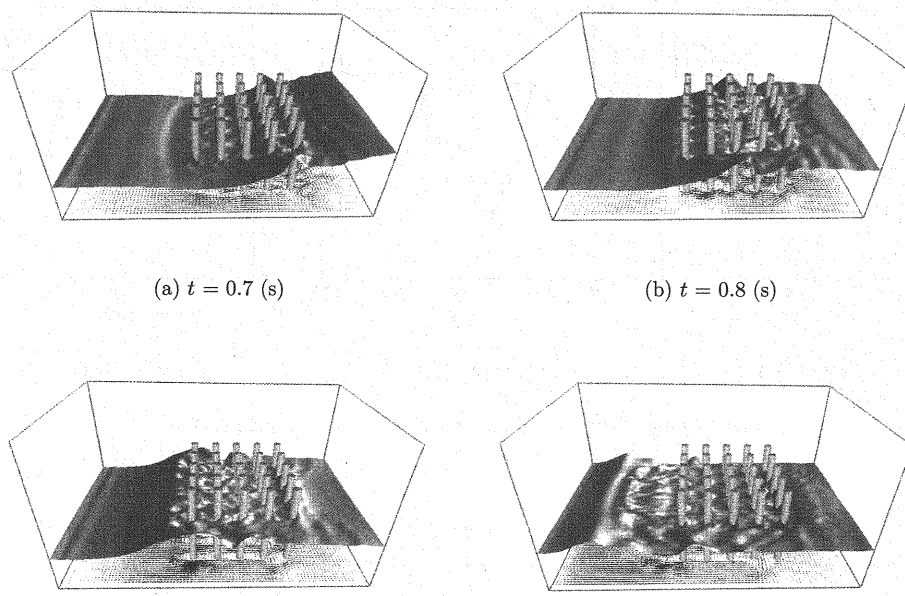

(a) $t = 0.7$ (s)

(b) $t = 0.8$ (s)

(c) $t = 0.9$ (s)

(d) $t = 1.0$ (s)

Fig. 6 Predicted results for case−5×5

Fig. 7 shows the comparisons of time histories of the fluid forces in the case−3×3, −4×4 and −5×5. The positive and negative peak values correspond to the maximum fluid forces caused by the wave-induced flows passing through the cylinders. While slight discrepancies are found in the phases and peak values of the time histories, the predicted results generally agree with the experiments. The difference of the phases are probably caused by the deformations in the supporting equipments except the steel plate, natural oscillations of the supporting system and other experimental errors. However, it can be seen that the unsteady fluid forces against the multiple cylinders, which are difficult to simulate with the usual computational methods, are satisfactorily predicted with the present method.

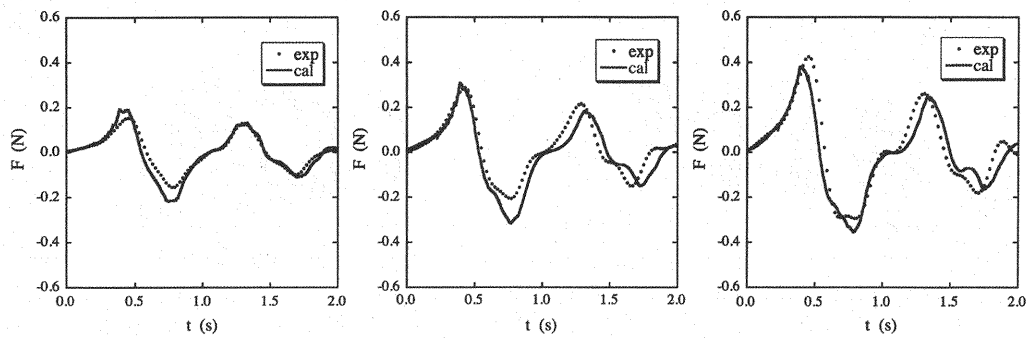

(a) case−3×3 (b) case−4×4 (c) case−5×5

Fig. 7 Time histories of fluid forces acting on rigid cylinders

Fig. 8 (a) shows the relationship between the total number of cylinders N and the maximum fluid forces F of the first wave-induced flows. It is shown that the relationship between N and F is approximately represented by a line through the origin in both experiments and predictions. On the other hand, the relationship between fluid forces per single cylinder F_e and N is shown in Fig. 8 (b). As shown in Fig. 8 (b), F_e is almost constant against N. From Figs. 8 (a) and (b), as far as the present experimental conditions are concerned, the shielding effects, in which the front objects attenuate the fluid forces acting on those located in the rear side, are not clearly recognized, since the tendency of decreasing fluid force against single cylinder is not obvious. While it was demonstrated that the present computational method is effective in predicting fluid forces against the group of cylinders, it might be necessary in further study to apply it to wider range of experiments in which N is larger than the present conditions in order to confirm its applicability to the shielding effects of multiple objects.

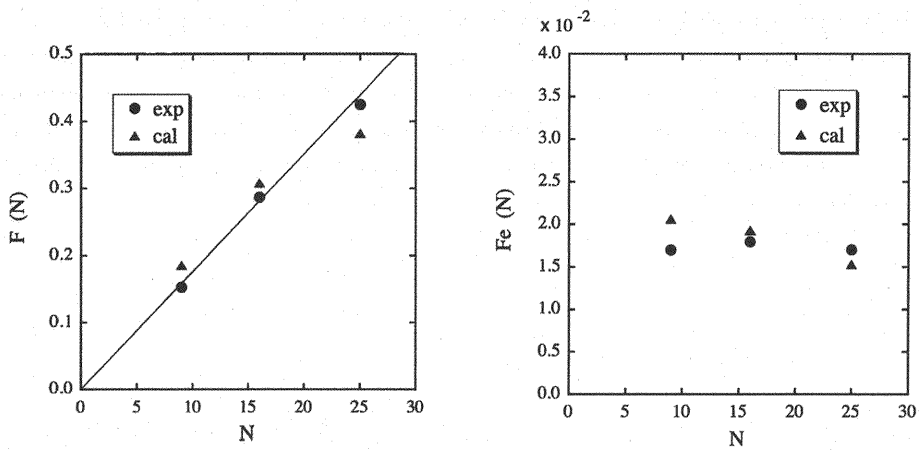

(a) Relationship between N and F (b) Relationship between N and F_e

Fig. 8 Comparisons of fluid force acting on cylinder

CONCLUSIONS

In this study, the applicability of a computational method for multiphase fields was investigated by applying it to the experimental results. The computational method, MICS, is based on a one-equation model for incompressible fluid-mixture and it enables us to deal with gas, liquid and solid phases by assuming that these phases are incompressible fluid-mixture. In order to confirm the applicability of the computational method, hydraulic experiments were carried out. In the experiments, a water tank equipped with multiple rigid cylinders was accelerated and the fluid forces caused by the generated wave-induced flows were measured by means of strain gages. By making comparisons between experiments and computations, it was demonstrated that the time histories of fluid forces acting on the group of cylinders, whose numbers are 9, 16 and 25, are reasonably predicted with only small differences in the phases and peak values. While the shielding effects were not clear both in experiments and predictions probably due to the lack of the cylinder numbers, the present computational method can be applied to estimate the fluid forces of free-surface flows acting on a group of cylindrical structures, which simply simulates the riparian vegetation along the river margins and the plants near coastal regions.

REFERENCES

1. Hayashi, K., Fujii, M. and Shigemura, T.: Fluid forces acting on multiple rows of circular cylinders in open-channel flow, *Annual Journal of Hydraulic Engineering, JSCE*, Vol. 45, pp. 475–480, 2001.

2. Ikeda, H. and Iwamatsu, Y.: Velocity profile variation by vertical structure of arboreal vegetation in rivers, *Journal of Applied Mechanics, JSCE*, Vol. 11, pp. 807–815, 2008.

3. Aburakawa, Y., Watanabe, Y., Ishida, Y., Igarasi, T., Tamadate, A., Suzuki, N. and Mitamura, K.: A field observation of flow velocity in trees during a flood, *Annual Journal of Hydraulic Engineering, JSCE*, Vol. 50, pp. 1159–1164, 2006.

4. Abe, S., Watanabe, Y. and Kuwamura, T.: Survey of vertical formation of flow velocity with riparian woods on 2005-flood in BIBAI river, *Annual Journal of Hydraulic Engineering, JSCE*, Vol. 50, pp. 1147–1152, 2006.

5. Okabe, T., Yamaguchi, Y. and Takebayashi, H.: Estimation of fluid resistance of riverine woody communities basing on velocity mesurements of natural wind, *Annual Journal of Hydraulic Engineering, JSCE*, Vol. 50, pp. 1153–1158, 2006.

6. Ushijima, S., Fukutani, A. and Makino, O.: Prediction method for movements with collisions of arbitrarily-shaped objects in 3D free-surface flows, *JSCE Journal*, Vol. 64/II-2, pp. 128–138, 2008.

7. Ushijima, S., Yamada, S., Fujioka, S. and Nezu, I.: Prediction method (3D MICS) for transportation of solid bodies in 3D free-surface flows, *JSCE Journal*, Vol. 810/II-74, pp. 79–89, 2006.

8. Ushijima, S., Takemura, M. and Nezu, I.: Investigation on computational schemes for MAC methods with collocated grid system, *JSCE Journal*, No. 719/II-61, pp. 11–19, 2002.

9. Ushijima, S. and Nezu, I.: Higher-order implicit (C-ISMAC) method for incompressible flows with collocated grid system, *JSCE Journal*, No. 719/II-61, pp. 21–30, 2002.

10. Yamamoto, S. and Daiguji, H.: Higher-order-accurate upwind schemes for solving the compressible Euler and Navier-Stokes equations, *Computers Fluids*, Vol. 22, No. 2/3, pp. 259–270, 1993.

11. Ushijima, S. and Okuyama, Y.: Comparison of C-HSMAC and SOLA methods for pressure computation of incompressible fluids, *JSCE Journal*, No. 747/II-65, pp. 197–202, 2003.

12. Nichols, B. D., Hirt, C. W. and Hotchkiss, R. S.: SOLA-VOF : A solution algorithm for transient fluid flow with multiple free boundaries, *Los Alamos Scientific Laboratory Report, LA-8355*, 1980.

13. Ushijima, S. and Kuroda, N.: Numerical method to predict interactions between free-surface flows and elastic bodies, *Proc. of Conf. On Modelling Fluid Flows (CMFF09)*, pp. 380–385, 2009.

APPENDIX-NOTATION

The following symbols are used in this paper:

B = width with a water tank;

C = a fluid cell;

D = diameter of a cylinder;

F = maximum fluid forces of the first wave-induced flows;

F^i_{Ckm} = fluid force acting on ΔT_{Ckm} in the x_i direction;

F_e = fluid forces per single cylinder;

L = length with a water tank;

L_0 = initial location of steel plate;

N = total number of cylinders;

RHS = right hand side of Eq. 6;

b = side length of a square acrylic plate;

d = distance between central axes of two neighboring cylinders;

f_i = acceleration component of external force;

g = gravity acceleration;

h_0 = initial water depth in tank;

l = axial length of a cylinder;

p = volume-averaged pressure;

t = time;

u_i = mass-averaged velocity component in the x_i direction;

x_i = orthogonal coordinates;

Ω = considering volume of whole multiphase field;

Ω_k = volume of phase$-k$ included in Ω;

α_{Ckm} = volume fraction;

$\delta_{i,j}$ = Kronecker's delta;

μ = volume-averaged coefficient of viscosity;

ρ = volume-averaged density;

ρ_b = density of the solid that occupies in a fluid cell; and

ρ_f = volume-averaged density in gas and liquid phases; and

ϕ^* = pressure deviation from the static pressure.

(Received Nov, 25, 2009 ; revised Sep, 01, 2010)